Proceedings Paper:
Gamble, A.S., Murison, R.A., Bowman, E.T. orcid.org/0000-0001-7868-6688 et al. (1 more author) (2025) Hydromechanical behaviour of a waste foundry sand. In: Cardoso, R., Jommi, C. and Romero, E., (eds.) E3S Web of Conferences. 5th European Conference on Unsaturated Soils and Biotechnology applied to Geotechnical Engineering (EUNSAT2025 + BGE), 01 Sep - 03 Jan 2025, Lisbon, Portugal. EDP Sciences ISSN: 2555-0403 EISSN: UNSPECIFIED

https://doi.org/10.1051/e3sconf/202564204007

Hydromechanical behaviour of a waste foundry sand

Alice S. Gamble[1], *Ruan* A. Murison[2], *Elisabeth* T. Bowman[1], and *Tiago* A.V. Gaspar[3*]

[1]The University of Sheffield, School of Mechanical, Aerospace and Civil Engineering, Sheffield S1 3JD, United Kingdom
[2]University of Pretoria, Department of Civil Engineering, Pretoria 0028, South Africa
[3]Imperial College London, Department of Civil & Environmental Engineering, London SW7 2AZ, United Kingdom

Abstract. Waste foundry sands are a byproduct of cast-metal processes. There is minimal geotechnical characterisation of these artificial soils in the literature, and as such their potential applications in construction have not been extensively explored. Due to the presence of coal and bentonite, their unsaturated properties, hydraulic behaviour, and mechanical response can be complex, and need to be better understood before assessing the feasibility for geotechnical applications. This study provides hydromechanical characterisation of a waste foundry sand in terms of soil-water retention, swelling, compression, and shear behaviour.

1 Introduction

1.1 Background

Waste foundry sand (WFS) is a byproduct of the metal sand casting process. This process involves the addition of a binder, usually bentonite clay or organic resins, to virgin silica sand for use as casting moulds [1]. WFS with clay binders, termed 'green sand', comprise 90% of the worldwide casting volume [2]. Green WFS is a mixture of uniform silica sand (85-95%), bentonite clay (4-16%), a coal additive (2-10%), and water (2-5%) [3]. A consequence of these constituents results in the categorisation of WFS as a mixture where the dominant behaviour is neither that of typical clay nor sand. As a result, its behaviour under loading is difficult to predict. The properties of WFS will depend on its composition, which will differ between foundries [4] and be dependent on the industry sector from which it originates. Whilst properties of WFS may vary between foundries, WFS samples from the same foundry will likely have consistent properties. Consequently, upon establishing parameters for a specific foundry, the feasibility for geotechnical or construction applications can be assessed.

1.2 Geotechnical uses of WFS

Geotechnical uses of WFS represent an opportunity to reuse significant quantities of material in high volume structural fill applications, which is crucial in preventing the tonnes of WFS being sent to landfills every year. WFS has been seen to perform as well as or better than natural sand or clay in a full-scale highway embankment field test, where only small deformations were recorded in all three materials [5]. A financial assessment of the project was also conducted, showing net savings of nearly USD 200 000 for the foundry compared to the disposal costs at the time. WFS could also be useful as a hydraulic barrier for waste disposal [6], achieving saturated hydraulic conductivities of $<10^{-9}$ m/s and being resistant to wet/dry cycling and freeze/thaw effects. WFS was considered a suitable pavement subbase material by [7] when compacted dry of optimum or at optimum moisture content. This study also highlighted the difference in mechanical behaviour of WFS between foundries.

1.3 Geotechnical properties of WFS

WFS is typically uniformly graded [8] with a coefficient of uniformity ranging between 0.9 and 1.5. The predominant grain shape is generally subangular or rounded. The fines content is seen to vary between foundries, with a higher bentonite content translating to a higher percentage fines. Furthermore, whilst clean sands are typically non-plastic, it has been shown that WFS plasticity varies with bentonite content [9], with contents >6% shown to provide significant plasticity. Such results indicate the vital effect that bentonite can have on the WFS behaviour. The maximum dry density (MDD) and optimum moisture content (OMC) measured using the standard proctor compaction method are generally reported between 1600-1850 kg/m^3 and 10-16%, respectively [10]. The saturated hydraulic conductivity, k_{sat}, has been seen to vary from 10^{-5} to 10^{-9} m/s and tends to decrease with increasing fines content. While shear strength properties of WFS have been shown to vary between foundries, measured values tend to be comparable to, or marginally lower than that of clean sands (i.e. $\phi' = 37°$ [11] and $\phi' \approx 28\text{-}31.8°$ [12]). The fines content within WFS is shown to be a significant factor controlling its mechanical behaviour, although no conclusive relationship has been provided in the literature. It was observed by [13] that a small addition of bentonite improves the WFS grading, increasing the MDD while decreasing the OMC. However, a large increase in fines

* Corresponding author: t.gaspar@imperial.ac.uk

content produces the opposite effect decreasing the MDD and increasing the OMC, a trend also observed by [4].

2 Material classification

WFS was obtained from a cast iron foundry located in Dronfield, United Kingdom. The soil is predominantly a silica sand, with a bentonite content of ~8.5% as reported by the supplier. The coal dust additive visibly coats all the sand and clay particles in the mixture. Due to the highly impermeable nature of the bentonite fraction of the WFS, all samples prepared in this study (for classification testing and element testing) were allowed to equilibrate in a sealed container for at least 24 hours. To avoid alteration of the plasticity in the clay fraction and oxidation of organic content in the coal fraction [14], oven-drying was avoided where possible. Where standards necessitated oven-dry soil, a lower temperature of 60°C (as opposed to the standard 105 C) was utilised.

Basic classification tests were performed in accordance with BS 1377 [15] to establish the soil's particle size distribution (PSD), maximum dry density and optimum moisture content ('ordinary', 2.5 kg hammer), the minimum dry density, and Atterberg limits of the soil. Additionally, the saturated hydraulic conductivity (k_{sat}) was investigated using the falling head test for soils of low permeability [16] using a sample compacted to a void ratio of 0.7. The test was repeated after four days of soaking to assess whether hydration of the clay particles significantly increased hydraulic conductivity with time. The PSD and material characteristics are presented in Figure 1 and Table 1 respectively.

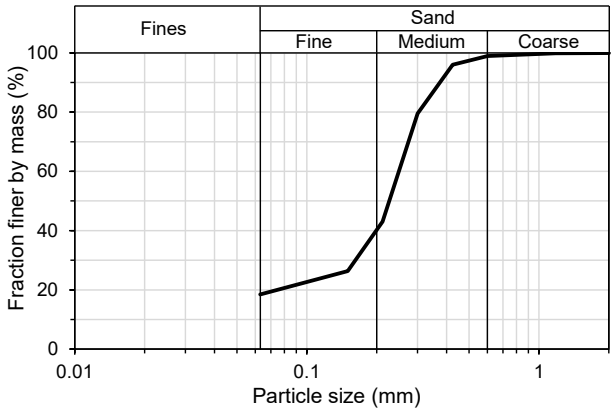

Fig. 1. Particle size distribution determined through wet sieving.

3 Soil-water retention behaviour

Soil-water retention and shrinkage curves in the high-suction range were established through discrete suction readings using a WP4C dewpoint hygrometer [17]. Samples were statically compacted (i.e. moist-tamped) using precision moulds, and wetting and drying were imposed by placing samples in desiccators with distilled water and silica crystals respectively, as described by [18].

Table 1. Index properties and classification to BS 1377 [15].

Property	Value
Specific gravity, G_s *	2.65
Mean particle diameter, d_{50} (mm)	0.226
Fines content (%)	19
Min. dry density, $\rho_{d,min}$ (kg/m^3)	1299
Max. dry density, $\rho_{d,max}$ (kg/m^3)	1660
Saturated hydraulic conductivity (falling head), k_{sat} (m/s)	7.5 x 10^{-8} (1 day) 5.7 x 10^{-8} (5 days)
Optimum moisture content (%)	14.0
Liquid limit (fall cone) (%)	42
Plastic limit (%)	26
Plasticity index (%)	16
BS Classification	SPu-CI

* Assumed

Initial sample dimensions were approximately 10 mm high and 15 mm in diameter. After each suction reading, the sample was weighed and 6 volumetric readings were taken with a vernier calliper, such that the water content, void ratio, and degree of saturation could be determined. Initial conditions for these samples are outlined in Table 2.

Table 2. Initial conditions for dewpoint hygrometer tests.

Sample no:	S1	S2	S3
Init. grav. water content, w_0 (%)	22.8	23.2	19.2
Initial void ratio, e_0	0.661	0.667	0.662
Init. deg. of saturation, S_0 (%)	91.4	92.0	77.1

After compaction, each sample was dried out to the maximum suction of the WP4C (300 MPa), after which it was wetted back to the initial water content. Hereafter, a second full drying and wetting cycle was applied for each sample. Satisfactory repeatability was shown between the tests, as highlighted by the first drying and wetting curves in Figure 2. Minor variations in shrinkage between samples were evident, but trends were similar. Note that only the first drying-wetting curves are presented for clarity, but similar repeatability was observed in the second drying-wetting cycles across the three samples.

Figure 3 shows the resulting soil-water retention curves (SWRCs) and shrinkage/swelling curves for one of the samples which underwent additional drying/wetting cycles. Bimodal water retention behaviour was exhibited during first drying, in each of the water content, degree of saturation, and void ratio projections of the SWRC in Figures 3a-c. This behaviour is typical of dual-structure materials, i.e. soils with bimodal pore size distributions, and has been observed for sand-bentonite mixtures in the literature (e.g. [19]). However, this bimodal shape was not evident during subsequent wetting and drying, and had seemingly 'collapsed' after initial drying to high suctions. After this collapse, the same void ratio vs suction path was followed during wetting and drying, with no significant hysteresis (Figure 3c). This preliminarily indicates that if a layer of compacted WFS for a geotechnical application is allowed to sufficiently dry out prior to wetting to the desired water content, seasonal wetting and drying of the

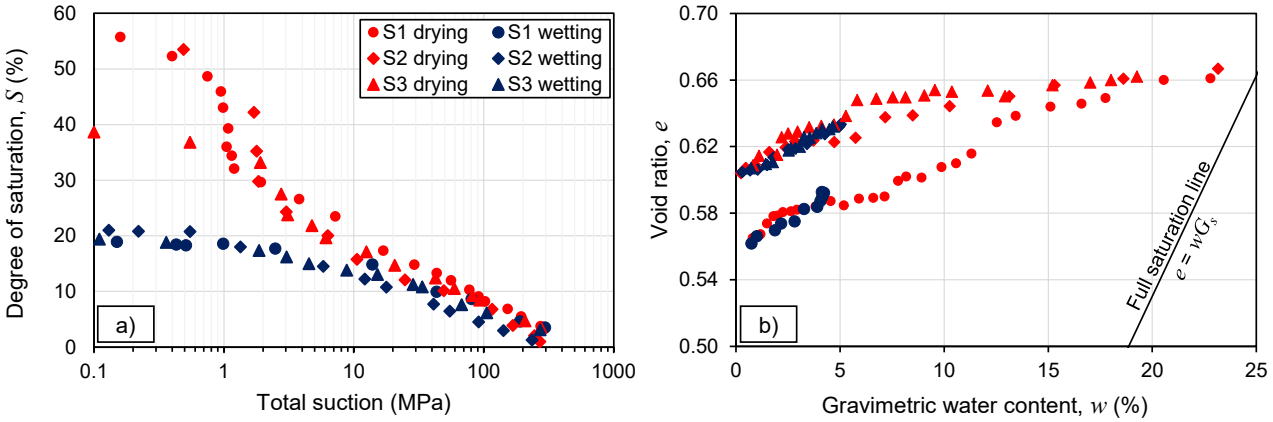

Fig. 2. First drying and wetting curves for all three samples.

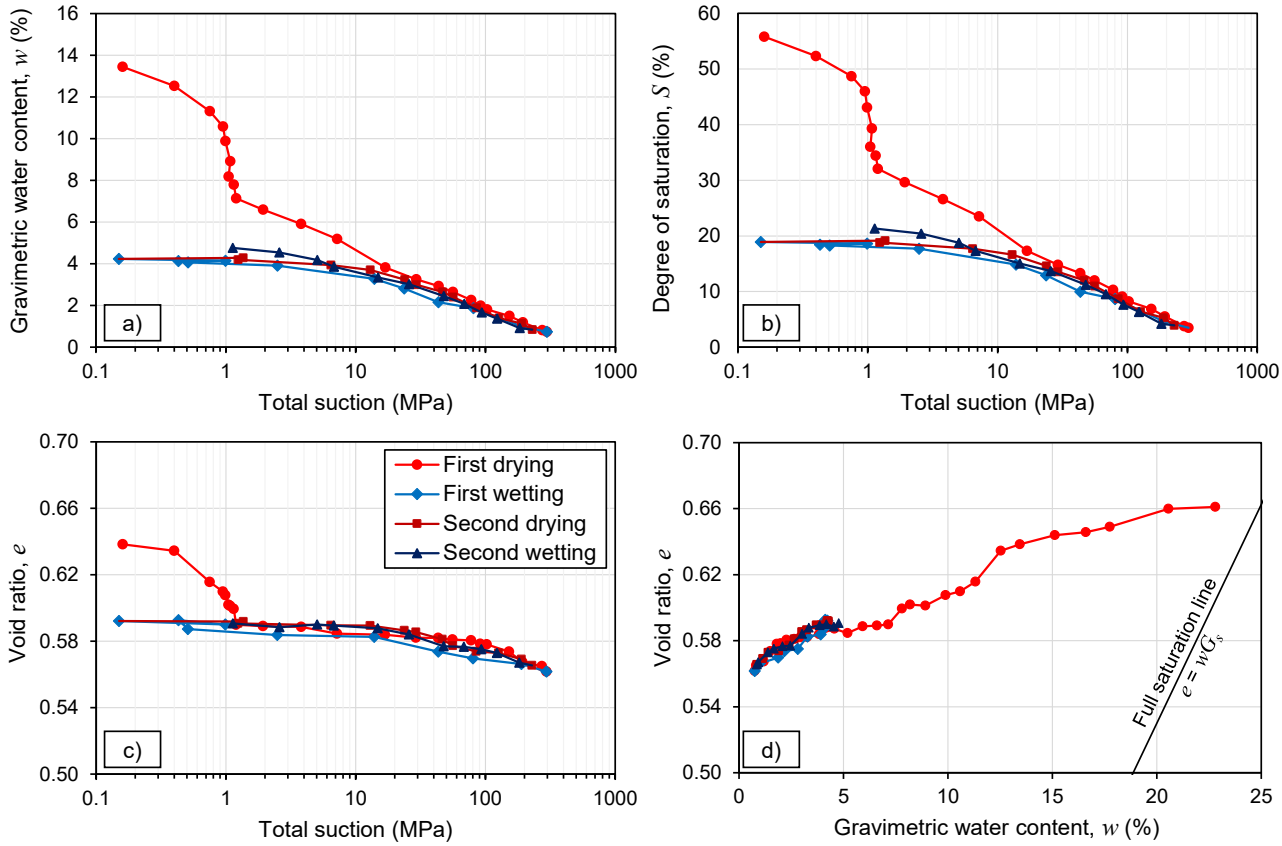

Fig. 3. Repeated drying and wetting soil-water retention and shrinkage/swelling curves for Sample S1.

layer is unlikely to lead to further accumulation of permanent volume change. Significant hysteresis in the water content and degree of saturation curves (Figures 3a and 3b) was observed between first drying and first wetting. However, no significant hysteresis was noted between the subsequent drying and wetting curves. Interestingly, no shrinkage limit could be observed in the first drying shrinkage curve (Figures 2b and 3d) as the void ratio continued to reduce during drying to water contents of less than 1%. Subsequent swelling and shrinkage curves followed along the same path as the first shrinkage curve, with no significant hysteresis (Figure 3d). Further investigation into the underlying mechanism driving this continuous volume change with decreasing water content, and lack of a shrinkage limit, is required.

4 Swelling and compression behaviour

To investigate the one-dimensional swelling behaviour of the waste foundry sand, moist-tamped oedometer samples were prepared to approximately the maximum dry density through static compaction with a hydraulic press. Standard 20 mm high and 75 mm diameter oedometer rings were used. A series of wetting after loading tests according to ASTM D4546 [20] were carried out to construct a swell-under-load curve, providing an indication of the swell potential under any given stress. After swelling was complete, the sample with the lowest soaking stress (12.5 kPa) was consolidated to high stresses, thus following the loading after wetting method according to ASTM D4546 [20]. The difference in void ratio between this compression curve and the initial void

ratio prior to soaking also represents the swell potential under a given vertical net stress ($\bar{\sigma}_v$). Initial conditions and measured swell potential ($-\varepsilon_{v,f}$) for each test are given in Table 3, and the swell-under-load and loading after wetting curves are given in Figure 4.

Table 3. Initial conditions for oedometer swell tests, and resulting swell potential values.

$\bar{\sigma}_v$ (kPa)	12.5	100	300	400	600
w_0 (%)	13.0	12.9	12.9	13.0	12.9
e_0	0.614	0.596	0.610	0.594	0.612
S_0 (%)	56.0	57.2	56.0	58.0	55.6
$-\varepsilon_{v,f}$ (%)	8.86	4.50	0.50	–0.21	–1.90

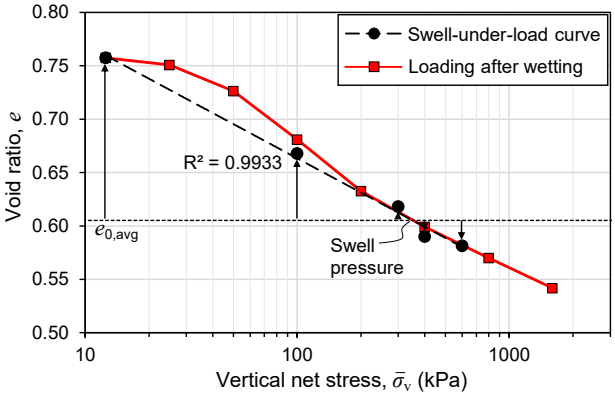

Fig. 4. One-dimensional swelling and consolidation behaviour.

The compression index (C_c) over the 200-1600 kPa range was determined to be 0.100. It is evident in Figure 4 that the swell potential predicted using the loading after wetting curve would be marginally higher than that from the swell-under-load curve for low stresses. For stresses greater than approximately 200 kPa, the curves practically coincided. The swell pressure of an expansive soil is defined as the stress required to fully restrain volume change. The vertical swell pressure can thus be read off from either of the curves at the intersection with the initial void ratio. Due to the approximate coincidence of the swell-under-load and loading after wetting curves, nearly identical swell pressures of 351 kPa and 353 kPa were recorded using the respective methods. This swell pressure is comparatively high, considering data in the literature on sand-bentonite mixtures with similar bentonite contents, compacted to maximum dry density at optimum moisture content. Swell pressures of 165 kPa for a 90/10 sand-bentonite mixture (i.e. 10% bentonite) and 580 kPa for a 70/30 mixture were reported by [21]. In another study [22], swell pressures ranging between 43 and 87 kPa were reported for a 90/10 sand-bentonite mixture, whilst swell pressures of 98 kPa, 171 kPa, and 270 kPa were reported for 80/20, 70/30, 50/50 mixtures respectively. In this case, even a 50% bentonite mix compacted to MDD generated a lower swell pressure than that of the waste foundry sand in the current study (<10% bentonite). Of course, this value would be highly dependent not only on the amount, but also the type of bentonite present (i.e. Na or Ca). The comparison of swell pressures serves as evidence of the highly expansive nature of the bentonite in this study's WFS.

Further comment on the nature of the bentonite in the WFS can be made when considering the development of swelling strain over time. Figure 5 shows the degree of swell (volumetric strain at any instant divided by the ultimate swelling strain), versus time. The swelling curve of the 12.5 kPa test in the current study was compared to a natural bentonitic expansive clay weathered from norite (after [23]), as well as two 90/10 sand-bentonite mixtures from literature, soaked under nominal vertical stresses. The water content condition at which the samples were compacted, as well as the soaking stress, are indicated in the legend. Each of the samples considered had an initial height of 20 mm, and two-way drainage. The comparatively slow time to equilibrium during swelling for the waste foundry sand (453 hours) highlights its low unsaturated hydraulic conductivity.

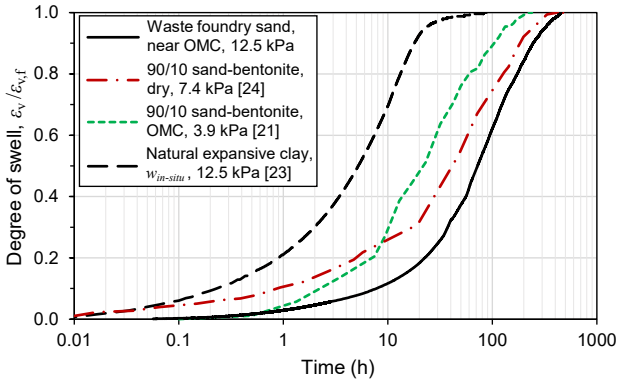

Fig. 5. Time to equilibrium during swelling for WFS, relative to soils from the literature.

5 Shear behaviour

To investigate the stress-strain and volumetric response during shearing, series of isotropically consolidated drained (CID) tests in triaxial compression were conducted on "loose" and "dense" moist-tamped samples. The target void ratios of the samples at compaction were 0.9 and 0.7 respectively. A hydraulic Bishop and Wesley stress path triaxial apparatus connected to three digital pressure controllers was utilised. Each 100 mm high × 50 mm diameter sample was prepared at optimum moisture content and statically compacted in five layers using the Ladd undercompaction method [25] to create samples of uniform density. Samples were flushed with CO_2 prior to saturation, and B-values of 95% were deemed satisfactory to confirm saturation prior to consolidation for all tests. The three samples in each set were subsequently consolidated to initial mean effective stresses (p_i') of 100, 200, and 300 kPa. Table 4 presents the sample conditions after compaction for the loose and dense tests, and the post-consolidation void ratios (e_i).

Coefficients of consolidation (c_v) ranging between 79 and 158 m^2/y were determined during the various consolidation phases. This corresponds with a minimum shear rate of 0.020%/min for drained shearing according to guidelines by [26], assuming failure occurs at 10% axial strain. However, this rate was found to be insufficiently slow to prevent the build-up of excess pore pressures. As a result, shearing rates were incrementally

reduced in each subsequent test. However, even when shearing an order of magnitude slower than the recommended rate, excess pore pressures developed in each of the tests, highlighting shortcomings of the guidelines for this abnormal soil. Figure 6 shows the buildup of excess pore pressure during shearing for all the tests. Due to the fact that shearing was not sufficiently slow to prevent the buildup of excess pore pressures, the effective stress paths and stress-strain curves reported in Figure 7 are thus for *partially drained* shearing. Although these stress paths are not standard, critical state properties and other valuable insights could still be gained.

Most notably, each of the dense samples exhibited contractive behaviour throughout shearing, as indicated by the volume reduction in Figure 7d-f, despite starting at significantly lower void ratios than the critical states attained by the loose samples. The buildup of positive excess pore pressures in Figure 6 also gives evidence of the contractive tendency for each of the samples. A unique critical state line projection could not be drawn in e-log p' space (Fig. 7d), as the void ratio at critical state was highly dependent on the initial void ratio, indicating transitional behaviour [27]. [3] suggested that a high bentonite content may suppress dilatant behaviour, potentially due to clay

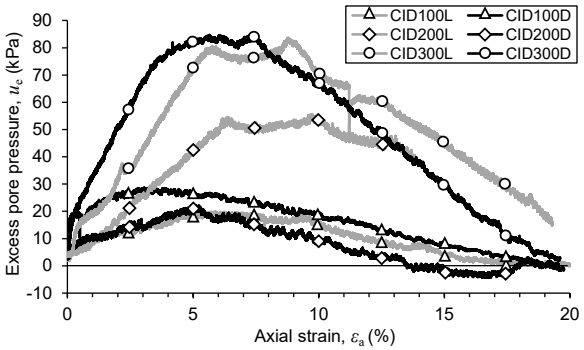

Fig. 6. Excess pore pressures during partially drained shearing.

coating large portions of the sand particles, allowing them to slide past rather than roll over each other during interparticle shearing. Similarly, the coal dust coating observed over all particles is likely to have reduced the coefficient of interparticle friction, as reported by [28]. An additional complexity arises from the contrasting hydraulic properties of coal and bentonite, which are respectively hydrophobic and hydrophilic. The interplay between these opposing characteristics may also have contributed to the unexpected buildup of excess pore pressures during shearing. However, further research is

Table 4. Summary of triaxial test conditions.

Test ID.	p_i' (kPa)	e_0	w_0 (%)	S_0 (%)	e_i	Shear rate (%/min)
CID100D	100	0.690	14.0	53.8	0.657	0.0075
CID200D	200	0.708	14.0	52.4	0.661	0.0020
CID300D	300	0.700	14.0	53.0	0.650	0.0055
CID100L	100	0.892	14.0	41.6	0.858	0.0035
CID200L	200	0.852	14.0	43.6	0.787	0.0025
CID300L	300	0.908	14.0	40.9	0.834	0.0025

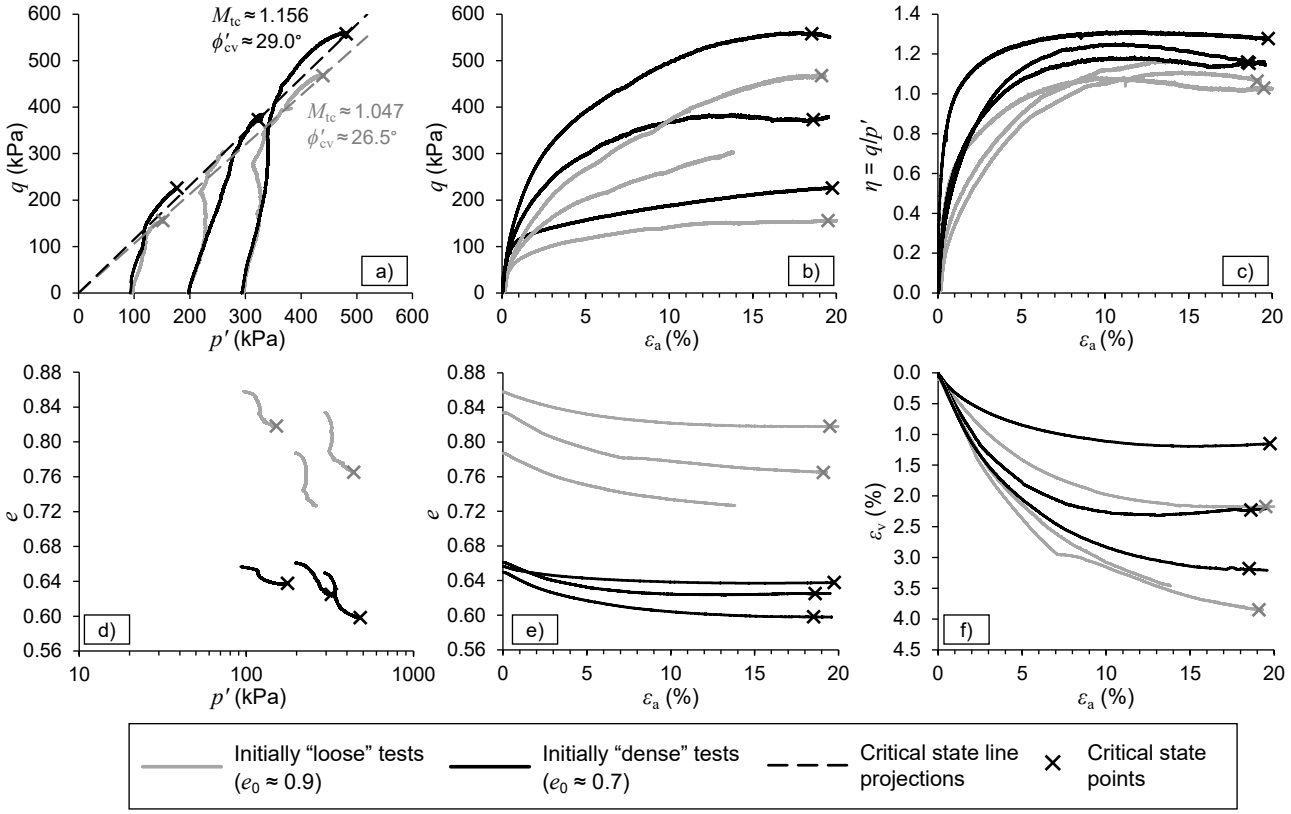

Fig. 7. Effective stress paths and stress-strain curves of waste foundry sand during partially drained shearing under triaxial compression.

required to confirm such an explanation.

The q-p' projection of the critical state line was also seemingly dependent on initial void ratio, with marginally greater shearing resistance mobilised for the dense tests (Figures 7a and 7c). Sample CID100D was marginally denser than the other samples in the dense set, and also exhibited greater shearing resistance compared to the dense CSL projection in Figure 7a. The critical state angles of shearing resistance (ϕ'_{cv}) of 26° and 29° are on the lower end of typical values for quartzitic sands, and slightly lower than values reported for WFS in the literature [11,12]. This may also be attributable to the reduction in interparticle friction due to the reasons mentioned previously.

6 Conclusions

Various aspects of the hydromechanical behaviour of a waste foundry sand were characterised in this study, and several features highlighting the non-textbook nature of the soil were observed. A bimodal SWRC in the megapascal range was observed during first drying, but collapsed onto a single curve for subsequent wetting and drying cycles. The tested samples did not encounter a shrinkage limit and continued to reduce in volume during drying to gravimetric water contents of less than 1%. The highly expansive nature of the bentonite fraction of the soil was evident in the high swell pressure (350 kPa) and slow equilibration time during swelling (453 hours under 12.5 kPa). Finally, the WFS can be classed as a transitional soil with no unique critical void ratio at a given effective stress. The void ratio at critical state was found to be highly dependent on initial void ratio, and all samples exhibited contractive behaviour throughout shearing. Shearing rates orders of magnitude slower than recommended guidelines would be required to ensure no excess pore pressure buildup during drained shearing. These phenomena were attributed to the coal and bentonite coating the sand particles, and the interplay between hydrophobic and hydrophilic fractions in the soil.

The authors would like to thank Jia Xiaoli for undertaking the unsaturated testing during her MSc project at the University of Sheffield, and Mr Mark Foster for his assistance with training and laboratory work. The second author gratefully acknowledges the Commonwealth Scholarship Commission for funding a year-long split-site scholarship tenure in Sheffield.

References

[1].P.J. Fox, D.G. Mast, Publication FHWA/IN/JTRP-98/18. Joint Transport. Res. Prog., Indiana Dept of Transport. & Purdue Univ., West Lafayette, (1998)

[2].F. Tittarelli. Eds. Siddique, R., Cachim, P., Waste and Suppl. Cement. Mat. in Concr.: Char., Prop., and Appl. Woodhead Publishing, pp. 121-147, (2018)

[3].J. Yin, A. Soleimanbeigi, W.J. Likos, T.B. Edil, J. Geotech. Geoenviron. Eng, **144**(2), (2018)

[4].M.J. Goodhue, T.B. Edil, C.H. Benson, J. Geotech. Geoenviron. Eng, **127**(4), pp. 353-362, (2001)

[5].B.K. Partridge, P.J. Fox, J.E. Alleman, D.G. Mast. Transp. Res. Rec., **1670**(1), pp. 98-105 (1999)

[6].T. Abichou, T.B. Edil, C.H. Benson, K.Tawfiq, *Recyc. Mat. in Geotech. Sess., ASCE Civ. Eng. Conf. & Expo*, Baltimore, Oct., pp. 186-200, (2004)

[7].J.R. Kleven, T.B. Edil, C.H. Benson, Transp. Res. Rec., **1714**(1), pp. 40-48, (2000)

[8].A. Deng, P. J. Tikalsky, J. Waste Manag, **28**, pp. 2161-2170, (2008)

[9].T. Abichou, C.H. Benson, T.B. Edil, J. Geotech. Geoenviron. Eng, **126**(12), pp. 1174-1183, (2000)

[10].A. Kumar, A. Parihar, Indian Geotech. J., **52**(2), pp. 416-436, (2022)

[11].A. Soleimanbeigi, T.B. Edil, J. Geotech. Geoenviron. Eng. **141**(5), pp. 1–14, (2015)

[12].E. Yaghoubi, A. Arulrajah, M. Yaghoubi, S. Horpibulsuk, Constr. Build Mater., **249**, 118761, (2020)

[13].S. Javed, FHWA/IN/JHRP-94/02J. Joint Highway Res. Proj., Indiana Dept. of Transport. & Purdue Univ., West Lafayette, (1994)

[14].K.H. Head, *Manual of Soil Laboratory Testing. Vol 1: Soil Classification and Compaction Tests*, London: Pentech Press, (1980)

[15].BSI, BS 1377:1990: Methods of test for soils for civil engineering purposes. BSI, London, UK, (1990).

[16].K.H. Head, *Manual of Soil Laboratory Testing. Vol 2: Permeability, Shear Strength and Compressibility Tests,* London: Pentech Press, (1982)

[17].Metergroup. *WP4C operator manual*, (n.d.)

[18].R.A. Murison, S.W. Jacobsz, T.A.V. Gaspar, T.S. da Silva Burke, A.S. Osman, E3S Web Conf., **382**, 09005, (2023)

[19].J.T. Stoicescu, M.D. Haung, D.G. Fredlund, *Proc. 2nd Intl. Conf. Unsat. Soils*, **1**, pp.143-148, (1998)

[20].ASTM, D4546 Standard Test Methods for One-Dimensional Swell or Collapse of Soils. ASTM, West Conshohocken, USA, (2021)

[21].A.S. Muntohar, Civ. Eng. Dim., **5**(2), pp. 93-98 (2003)

[22].H. Komide, N. Ogata, Soils & Foundations, **39**(2), pp. 83-97, (1999)

[23].T.A.V. Gaspar, S.W. Jacobsz, G. Heymann, D.G.Toll, A. Gens, A.S. Osman. Eng. Geol., **303**, 106607, (2022)

[24].L.H. Mollins. PhD thesis, Univ. of Leeds, (1996)

[25].R.S. Ladd, Geotech. Test. J, **1**(1), pp. 16-23, (1978)

[26].K.H. Head, R.J. Epps, *Manual of Soil Laboratory Testing. Vol 3: Effective Stress Tests 3rd edn*, Caithness: Whittles Publishing, (2014)

[27].V. A. Rinaldi et al., *Proc. 6th Intl Conf Def. Charac. Geomat.,* Buenos Aires, November, (2015)

[28].J. Chen, R. Gao, Y. Liu, Z. Shi, R. Zhang, Construct. Build. Mat., **273**, 121927, (2021)